



## Effects of Mg<sup>2+</sup> addition on structure and electrical properties of gadolinium doped ceria electrolyte ceramics

Jihai Cheng\*, Changan Tian, Jie Yang

Department of Chemistry and Materials Engineering, Hefei University, Hefei 230601, China

Received 4 December 2018; Received in revised form 27 February 2019; Accepted 22 May 2019

### Abstract

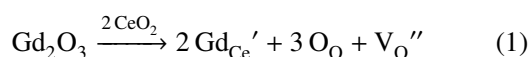
Series of Gd<sup>3+</sup> and Mg<sup>2+</sup> co-doped ceria (Ce<sub>0.8</sub>Gd<sub>0.2-x</sub>Mg<sub>x</sub>O<sub>1.9-δ</sub>) powders were prepared by a sol-gel method and electrolyte ceramics were obtained by sintering at 1300 °C. Thermogravimetric and differential scanning calorimetry, X-ray diffraction, scanning electron microscope and electrochemical impedance spectroscopy were used for structural, morphology and electrical characterization of the prepared samples. Well crystalline cubic fluorite structured composite was confirmed after calcination at 700 °C and the electrolyte ceramics sintered at 1300 °C for 4 h was quite dense with uniform microstructure. The electrochemical analysis results displayed that the highest conductivity has the Ce<sub>0.8</sub>Gd<sub>0.14</sub>Mg<sub>0.06</sub>O<sub>1.87</sub> compound, i.e. 0.0203 S/cm at 800 °C. Therefore, it was concluded that co-doping with Gd<sup>3+</sup> and Mg<sup>2+</sup> could enhance the electrical properties of the CeO<sub>2</sub> based solid electrolytes.

**Keywords:** ceramic electrolytes, co-doping, ceria, electrical properties

### I. Introduction

Solid oxide fuel cell (SOFC) has been studied deeply as an advanced future renewable energy device due to its high-efficiency energy conversion and environmental friendliness [1–4]. Electrolyte plays the most important role in SOFC, as it determines the operating temperature to a large extent.

CeO<sub>2</sub>-based electrolytes attracted considerable attention as their oxygen ion conductivity in intermediate temperature range (600–800 °C) is higher than that for yttria stabilized zirconia (YSZ). The conductivity can be even increased by doping with trivalent rare earth ions. When ceria is doped with rare earth and alkaline earth cations, oxygen vacancy is formed to compensate the charge balance in the lattice [5]. The defect reaction equation is as follows:



The rare earth and alkaline earth ions (Gd<sup>3+</sup>, Sm<sup>3+</sup>, Y<sup>3+</sup>, Ca<sup>2+</sup> and Sr<sup>2+</sup>) doped ceria at different concentrations have been extensively studied as an upcoming alterna-

tive solid electrolyte to YSZ [6–10]. Among them, Gd<sup>3+</sup> doped ceria (GDC) is considered as promising electrolyte material due to its high oxygen ion conductivity, low polarization resistance and compatibility with electrodes [5,11].

Recently, co-doping with two or more aliovalent cations has been reported as more efficient strategy [12–17]. Muhammed Ali's finding [18] confirmed that ionic conductivity of multi-doped ceria (Ce<sub>0.8</sub>Sm<sub>0.1</sub>Ba<sub>0.05</sub>Er<sub>0.05</sub>O<sub>2-δ</sub>) is considerably influenced by dopant radius and sintering temperatures with respect to surface morphology, microstructure and oxygen vacancy radius. Co-doped ceria was studied by Arabaci [19], who showed that Ce<sub>0.9-x</sub>Gd<sub>0.1</sub>Er<sub>x</sub>O<sub>1.9-x/2</sub> materials can be used as electrolytes for IT-SOFC applications instead of GDC. Maheshwari [7] found that Sr<sup>2+</sup>-Gd<sup>3+</sup> co-doped CeO<sub>2</sub> samples show significantly higher total electrical than the electronic conductivities which recommended them as good materials for SOFC electrolytes. The addition of 1 mol% CuO in gadolinium doped ceria showed no detrimental effect on the total electrical conductivity [20].

In view of the above discussions, in the present investigation, gadolinium and magnesium co-doped ceria powders were prepared by a sol-gel route. The effects of Mg addition on the properties of ceria

\*Corresponding authors: tel: +86 551 62158442, e-mail: [cjh@hfu.edu.cn](mailto:cjh@hfu.edu.cn)

based electrolytes, the structure and the conductivity of  $\text{Ce}_{0.8}\text{Gd}_{0.2-x}\text{Mg}_x\text{O}_{1.9-\delta}$  samples were investigated.

## II. Experimental

### 2.1. Sample preparation

Ultrafine  $\text{Ce}_{0.8}\text{Gd}_{0.2-x}\text{Mg}_x\text{O}_{1.9-\delta}$  powders ( $x = 0, 0.02, 0.04$  and  $0.06$ ) were prepared by a sol-gel method. In this process, analytical pure cerium nitrate ( $\text{Ce}(\text{NO}_3)_3 \cdot 6\text{H}_2\text{O}$ , containing 39 wt.% of  $\text{CeO}_2$ ), gadolinia ( $\text{Gd}_2\text{O}_3$ , 99.99 wt.%), magnesium nitrate ( $\text{Mg}(\text{NO}_3)_2 \cdot 2\text{H}_2\text{O}$ , analytical reagent) were used as starting materials. All raw materials were purchased from the China National Medicines Corporation Ltd. The experimental flowchart of  $\text{Ce}_{0.8}\text{Gd}_{0.2-x}\text{Mg}_x\text{O}_{1.9-\delta}$  preparation using the sol-gel method is shown in Fig. 1. The stoichiometric amount of precursors were dissolved in deionized water and mixed together. Citric acid was then added as complexing agents to form a homogeneous solution, the molar ratio of citric acid to metal ions was 1.5 : 1. The obtained mixture was continuously stirred using a magnetic agitator to form a homogeneous solution at  $80^\circ\text{C}$  and then converted to a viscous gel.

The synthesized  $\text{Ce}_{0.8}\text{Gd}_{0.2-x}\text{Mg}_x\text{O}_{1.9-\delta}$  powders were uniaxially pressed into discs of 11 mm in diameter and 0.5 mm in thickness under a pressure of 200 MPa. Finally, the green discs were sintered in a high-temperature furnace at  $1300^\circ\text{C}$  for 4 h.

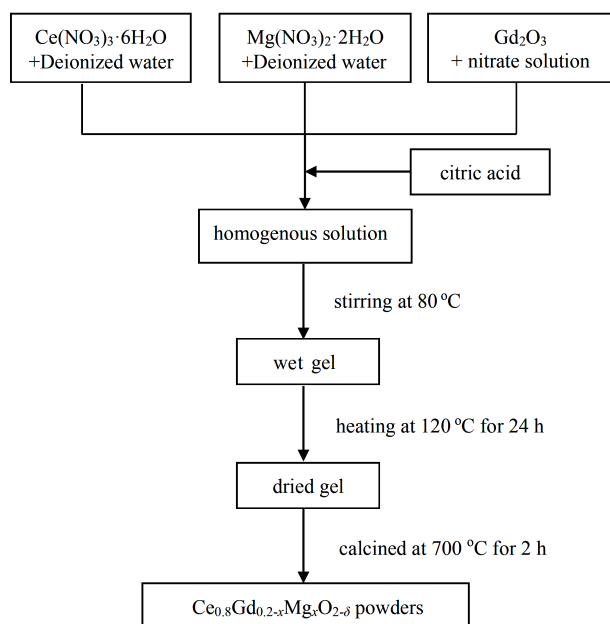


Figure 1. Experimental flowchart of preparation of samples by the sol-gel method

### 2.2. Characterization

The xerogels were studied by simultaneous thermogravimetric and differential scanning calorimetry (TG-DSC) (Netzsch STA 409PC, Germany) under a flow of air at a rate of  $10^\circ\text{C}/\text{min}$ . The phase of the calcined powders was analysed by X-ray diffraction (XRD,

Rigaku, Japan). Scans were taken with a  $2\theta$  step of  $0.02^\circ$  (over the range of  $20\text{--}80^\circ$ ) using  $\text{Cu K}\alpha$  radiation ( $18\text{ kV}$ ,  $\lambda = 0.154056\text{ nm}$ ). The microstructure was analysed with a scanning electron microscope (SEM, Model S4800). By using alternating-current impedance spectroscopy (Model CHI660D, China), the conductivity of the specimens was measured over the temperature range of  $500$  to  $800^\circ\text{C}$  in air. Before measurements, Ag paste was painted onto either side of the discs and fired at  $700^\circ\text{C}$  for 30 min to erase the solvent. Data were collected in the frequency range  $0.1\text{ Hz--}100\text{ kHz}$ ; registered impedance spectra were analysed using ZSimpWin software.

## III. Results and discussion

### 3.1. TG-DSC analysis

Figure 2 shows TG-DSC plots of the dried  $\text{Ce}_{0.8}\text{Gd}_{0.14}\text{Mg}_{0.06}\text{O}_{1.87}$  precursor gel measured in temperature range from  $50$  to  $700^\circ\text{C}$  in air atmosphere. An initial weight loss of 30 wt.% below  $300^\circ\text{C}$  was seen in Fig. 2 which correlated with the evaporation of the adsorbed water and the decomposition of organics such as citric acid. A dramatic weight loss of  $\sim 30\text{ wt.}\%$  can be observed in the temperature range  $300\text{--}380^\circ\text{C}$  accompanied by an intense exothermic peak in the DSC curve, which can be attributed to the decomposition of organic groups and  $\text{NO}_3^-$ . At the temperatures above  $380^\circ\text{C}$ , there is no remarkable changes in TG curve. However, in DSC curve a wide exothermic peak ( $500\text{--}650^\circ\text{C}$ ) can be detected, indicating that the phase transition and crystallization of the sample have happened. Thus, we selected  $700^\circ\text{C}$  as the calcination temperature of the synthesised  $\text{Ce}_{0.8}\text{Gd}_{0.2-x}\text{Mg}_x\text{O}_{1.9-\delta}$  powders, as it is sufficient to obtain the desired crystalline structure.

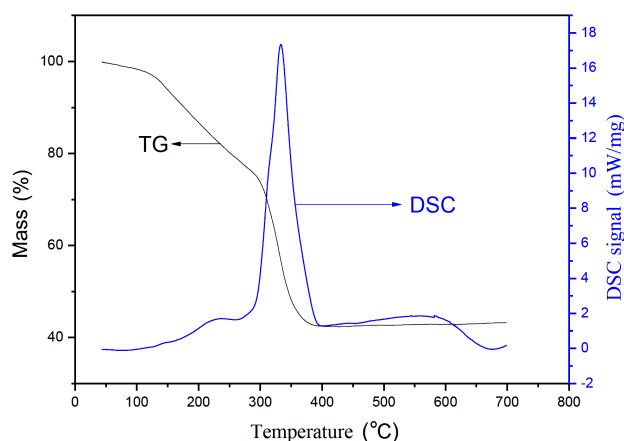


Figure 2. TG-DSC curves of  $\text{Ce}_{0.8}\text{Gd}_{0.14}\text{Mg}_{0.06}\text{O}_{1.87}$  xerogel

### 3.2. Phase structure

Figure 3 shows the XRD patterns of the  $\text{Ce}_{0.8}\text{Gd}_{0.14}\text{Mg}_{0.06}\text{O}_{1.87}$  ( $x = 0.06$ ) powders calcined at  $500$ ,  $600$  and  $700^\circ\text{C}$  for 2 h. The typical diffraction peaks of cubic fluorite structure occurred

at 500 °C, but the intensity of the diffraction peaks was weak, and some characteristic peaks were not observed. This indicates that the sample was not well crystallized at this temperature. When the calcination temperature increased to 700 °C, the appearance of the typical diffraction peaks indicated that the powders

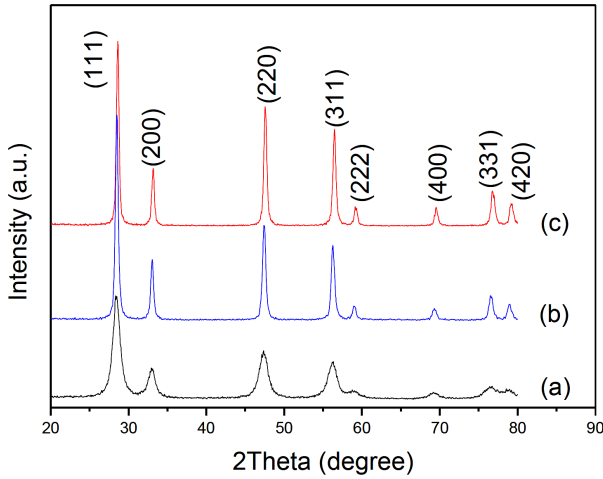


Figure 3. XRD patterns of the  $\text{Ce}_{0.8}\text{Gd}_{0.14}\text{Mg}_{0.06}\text{O}_{1.87}$  powders calcined at: a) 500, b) 600 and c) 700 °C

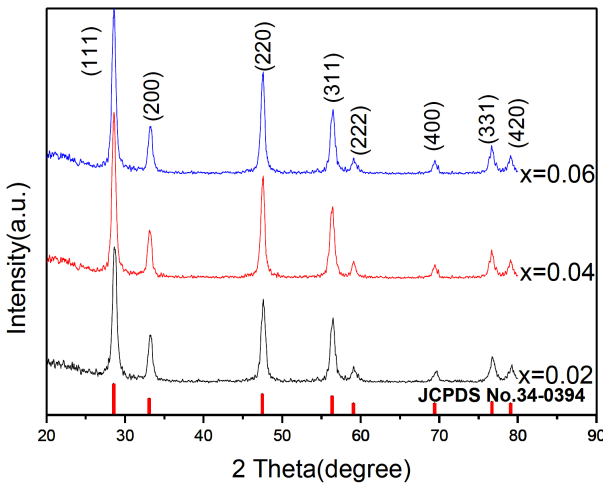


Figure 4. XRD patterns of  $\text{Ce}_{0.8}\text{Gd}_{0.2-x}\text{Mg}_x\text{O}_{1.9-d}$  with different dopant concentrations

crystallized well and formed cubic fluorite structure with space group  $Fm\bar{3}m$  of  $\text{CeO}_2$  (PDF No. 34-0394). Thus, fine  $\text{Ce}_{0.8}\text{Gd}_{0.14}\text{Mg}_{0.06}\text{O}_{1.87}$  powders with cubic fluorite-type structure were successfully prepared after calcined at 700 °C for 2 h, which was consistent with the TG-DSC results.

XRD patterns for the samples with different Mg-dopant concentrations are shown in Fig. 4. All powders calcined at 700 °C have a single-phase fluorite structure. It can be seen that no secondary phase could be identified. According to previous studies, doping with ions having different valences and different ionic radii will change the lattice parameter of ceria and induce corresponding oxygen vacancies generate the internal stress in the ceria matrix [21–23]. The lattice parameters of the prepared  $\text{Ce}_{0.8}\text{Gd}_{0.2-x}\text{Mg}_x\text{O}_{1.9-d}$  samples are basically not changed considerably with the Mg-doping concentration, and remained  $a = b = c = 0.5418$  nm. This observation could indicate that solubility of  $\text{Mg}^{2+}$  in the GDC lattice is very low. The reason could be the difference in ionic radii of  $\text{Mg}^{2+}$  (0.089 nm) and  $\text{Ce}^{4+}$  (0.097 nm). Thus, the addition of Mg might cause a distortion of the lattice as well as the increase of lattice energy.

### 3.3. Microstructure analysis

Micrographs of the  $\text{Ce}_{0.8}\text{Gd}_{0.14}\text{Mg}_{0.06}\text{O}_{1.87}$  ceramics sintered at 1300 °C for 4 h are shown in Fig. 5. As can be seen, the density of the sample sintered at 1300 °C is high and the grains are connected to each other with only few pores visible. As the addition of  $\text{Mg}^{2+}$  increases, the change in density is not significant, the average grain size was in the range of 1–2 μm.

It was reported that ceria electrolytes with density above 95% of theoretical density were produced by sintering at 1200 or 1250 °C [20,24,25]. However, for densification of the Mg-doped GDC the sintering temperature of 1300 °C was necessary. The reason could be that  $\text{Mg}^{2+}$  is not dissolved into GDC completely, but enriched partially the grain boundaries of the samples. The high melting point of the MgO phase (~2852 °C) and the low solubility of  $\text{Mg}^{2+}$  [17], could give some support to this idea. However, phase structure analysis indicates that there is no formation of any new phase.

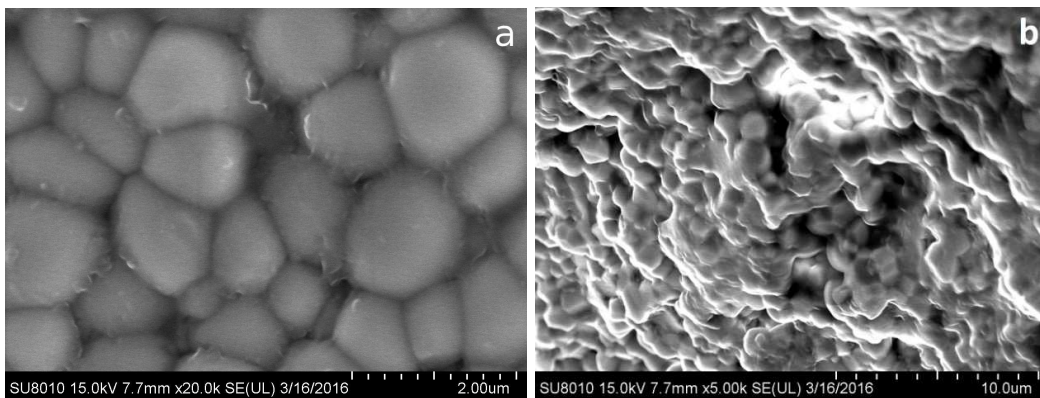


Figure 5. SEM images for  $\text{Ce}_{0.8}\text{Gd}_{0.14}\text{Mg}_{0.06}\text{O}_{1.87}$  sintered at 1300 °C for 4 h in air: a) surface and b) fresh fracture

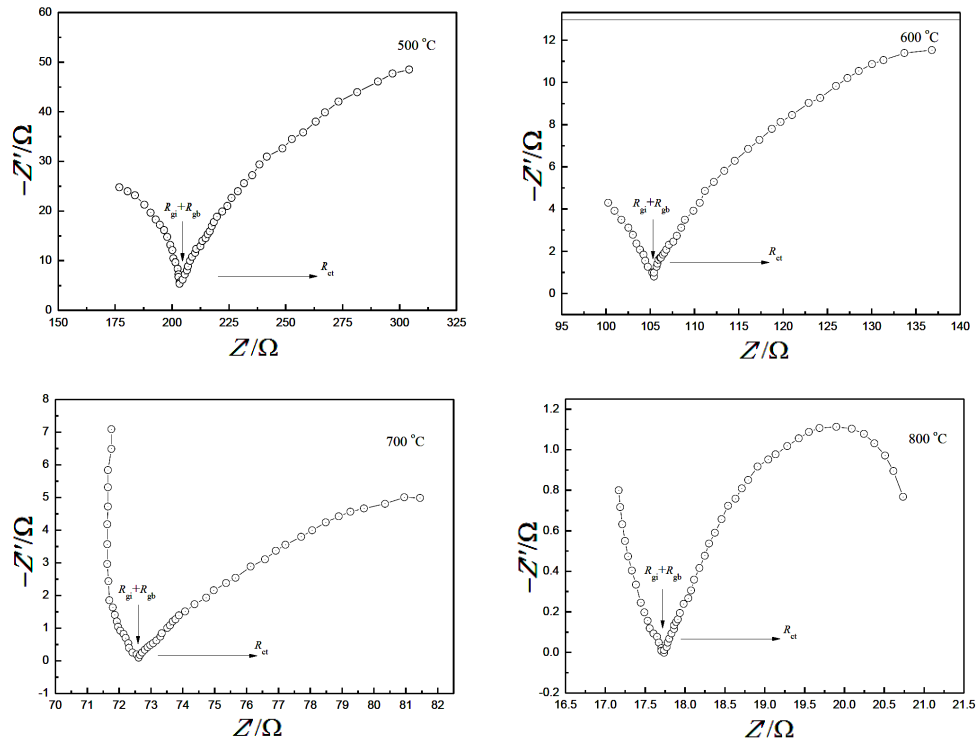


Figure 6. Impedance spectra of  $\text{Ce}_{0.8}\text{Gd}_{0.18}\text{Mg}_{0.02}\text{O}_{1.9-\delta}$  ( $x = 0.02$ ) tested at different temperatures

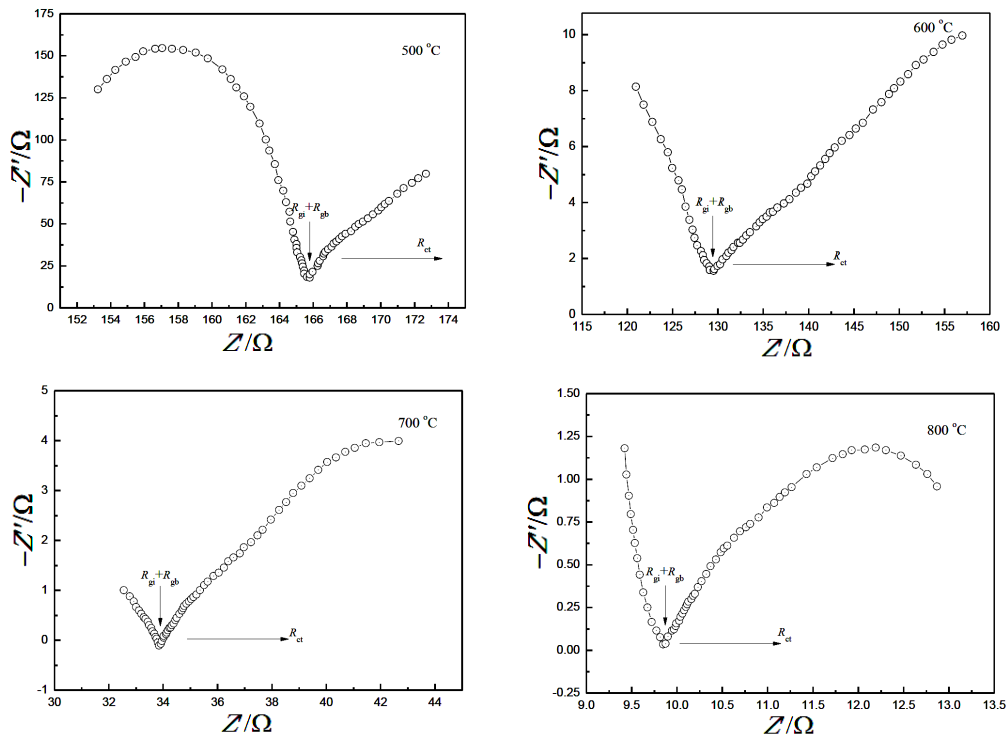


Figure 7. Impedance spectra of  $\text{Ce}_{0.8}\text{Gd}_{0.14}\text{Mg}_{0.06}\text{O}_{1.9-\delta}$  ( $x = 0.06$ ) tested at different temperatures

This demonstrates that the content of undissolved MgO at the grain boundaries, if exists, is lower than the detection limits of X-ray diffraction.

### 3.4. Electrochemical performance

Electrochemical impedance spectroscopy (EIS) has been used to determine electrochemical properties of the

solid electrolyte. From the impedance spectroscopy, it is possible to obtain the information on the contribution of grains, grain boundaries and electrode polarization to the total conductivity [25–27]. Impedance spectra for the  $\text{Ce}_{0.8}\text{Gd}_{0.2-x}\text{Mg}_x\text{O}_{1.9-\delta}$  ceramics measured at different temperatures under air are presented in Figs. 6 and 7. The conductivities can be calculated from the resis-

**Table 1. Conductivity and correlative parameters of the samples at different temperatures**

<i>x</i>	<i>L</i> [cm]	<i>S</i> [cm <sup>2</sup> ]	<i>R</i> <sub>tot</sub> [Ω]				<i>σ</i> [S/cm]			
			500 °C	600 °C	700 °C	800 °C	500 °C	600 °C	700 °C	800 °C
0	0.108	1.18	91.62	21.28	6.72	6.43	9.9×10 <sup>-4</sup>	0.0043	0.0136	0.0142
0.02	0.118	1.09	188.11	109.47	74.55	17.72	5.8×10 <sup>-4</sup>	9.9×10 <sup>-4</sup>	0.0015	0.0061
0.04	0.11	1.13	261.7	124.52	83.30	12.78	4.08×10 <sup>-4</sup>	7.82×10 <sup>-4</sup>	0.0012	0.0076
0.06	0.114	1.11	86.41	30.13	6.51	5.05	0.0019	0.0034	0.0158	0.0203

**Table 2. Conductivity and activation energy of co-doped CeO<sub>2</sub> electrolytes at 800 °C**

Composition	Reference	Total ionic conductivity	Conductivity activation energy
		[S/cm]	[eV]
Ce <sub>0.8</sub> Gd <sub>0.18</sub> Mg <sub>0.02</sub> O <sub>1.9-δ</sub>	Present work	0.0061	0.972
Ce <sub>0.8</sub> Gd <sub>0.14</sub> Mg <sub>0.06</sub> O <sub>1.9-δ</sub>	Present work	0.0203	0.853
(CeO <sub>2</sub> ) <sub>0.92</sub> (Y <sub>2</sub> O <sub>3</sub> ) <sub>0.02</sub> (Gd <sub>2</sub> O <sub>3</sub> ) <sub>0.06</sub>	[8]	0.042	0.664
Ce <sub>0.82</sub> Gd <sub>0.1</sub> Er <sub>0.08</sub> O <sub>1.86</sub>	[19]	0.0357	0.804
Ce <sub>0.85</sub> Sr <sub>0.05</sub> Gd <sub>0.1</sub> O <sub>2-δ</sub>	[7]	0.0635	1.13
Ce <sub>0.8</sub> Sm <sub>0.15</sub> Sc <sub>0.05</sub> O <sub>2-δ</sub>	[20]	0.0192	1.106

tance obtained by fitting the impedance spectra using ZSimpWin software. Then the conductivities at different temperatures can be obtained using the equation:

$$\sigma = \frac{L}{R \cdot S} \quad (2)$$

where *L* is the sample thickness and *S* is the electrode area of the sample.

Conductivity and resistance values of the samples at different temperatures are listed in Table 1. A minor decrease in conductivity was observed in the samples with low Mg-concentration (*x* = 0.02 and 0.04). However, the increase in conductivity was observed when the dopant content increases to *x* = 0.06 reaching 0.0203 S/cm at 800 °C. The reason may be that with the increasing of Mg content, the oxygen vacancies are more mobile which results in the increased conductivity [28]. Incorporation of Mg into GDC lattice enhanced the oxygen ionic conductivity also through the increasing of the number of oxygen vacancies. Thus, the more incorporated dopant means the more oxygen vacancies, but in the same time the migration of the oxygen ions is hindered due to the shrinkage of the lattice [19]. Therefore, the sample doped with 6 mol% Mg<sup>2+</sup> showed the highest ionic conductivity. Table 2 shows the conductivities and activation energies of co-doped CeO<sub>2</sub> electrolytes at 800 °C. It can be seen that the conductivity and the activation energy of Mg<sup>2+</sup>-doped GDC are close to that of other single or double-doped CeO<sub>2</sub> electrolytes, indicating that Ce<sub>0.8</sub>Gd<sub>0.2-x</sub>Mg<sub>x</sub>O<sub>1.9-δ</sub> is a promising electrolyte for intermediate-temperature SOFC.

The total electrical conductivity of Ce<sub>0.8</sub>Gd<sub>0.2-x</sub>Mg<sub>x</sub>O<sub>1.9-δ</sub> can be described in terms of the relationship of ln(*σ* · *T*) versus 1000/*T*, as plotted in Fig. 8 over the temperature range 500–800 °C. As can be seen from Fig. 8, the relationship between conductivity and temperature of Ce<sub>0.8</sub>Gd<sub>0.2-x</sub>Mg<sub>x</sub>O<sub>1.9-δ</sub>

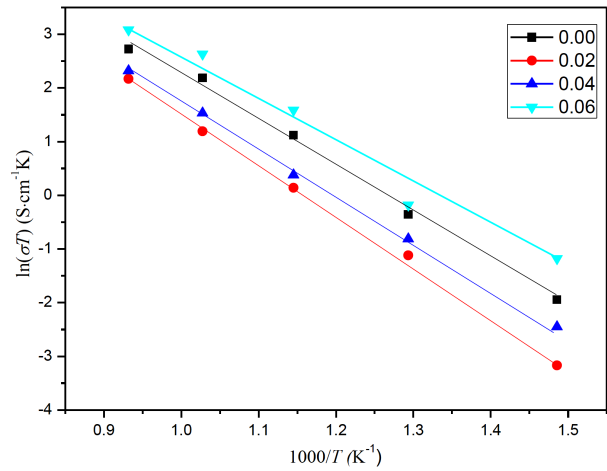


**Figure 8. Arrhenius plots comparing the total conductivity of Ce<sub>0.8</sub>Gd<sub>0.2-x</sub>Mg<sub>x</sub>O<sub>1.9-δ</sub> electrolytes**

obeyed the Arrhenius relation:

$$\sigma = \frac{A}{T} \exp\left(-\frac{E_a}{K \cdot T}\right) \quad (3)$$

where *σ* is the conductivity of the sample, *E<sub>a</sub>* is the conduction activation energy, *K* is Boltzmann constant and *T* is the absolute temperature. The conductivity activation energy of Ce<sub>0.8</sub>Gd<sub>0.14</sub>Mg<sub>0.06</sub>O<sub>1.87</sub> is calculated to be 0.853 eV.

Overall, analysis results suggest that Mg may be used as a co-dopant for the optimization of electrical properties of Ce<sub>0.8</sub>Gd<sub>0.2</sub>O<sub>1.9</sub> based electrolytes. This indicated that Ce<sub>0.8</sub>Gd<sub>0.2-x</sub>Mg<sub>x</sub>O<sub>1.9-δ</sub> is a possible electrolyte material for IT-SOFC.

#### IV. Conclusions

Ce<sub>0.8</sub>Gd<sub>0.2-x</sub>Mg<sub>x</sub>O<sub>1.9-δ</sub> powders (*x* = 0, 0.02, 0.04 and 0.06) were synthesized by the sol-gel method and sin-

tered at 1300 °C. XRD analysis confirmed the single-phase fluorite structure can be formed at a relatively low calcination temperature. SEM observations confirmed that the electrolytes sintered at 1300 °C for 4 h have dense structure. Based on the EIS data, the co-doped electrolyte with 6 mol% MgO content has the highest conductivity, i.e. 0.0203 S/cm at 800 °C. It is believed that the oxygen vacancies are activated when GDC is doped with Mg<sup>2+</sup>, causing the increase of conductivities of the Ce<sub>0.8</sub>Gd<sub>0.14</sub>Mg<sub>0.06</sub>O<sub>1.87</sub> electrolyte in comparison to the Gd singly doped CeO<sub>2</sub> electrolytes. Thus, co-doping with Mg led to an improvement in conductivity confirming that Ce<sub>0.8</sub>Gd<sub>0.2-x</sub>Mg<sub>x</sub>O<sub>1.9-δ</sub> is a possible electrolyte material for IT-SOFC.

**Acknowledgement:** This work has been supported by the Natural Science Foundation of Education Department of Anhui Province under contract No. KJ2016A591 and KJ2018A0549, the Nature Science Foundation of Anhui Province of China under contract No. 1708085ME112, and the Natural Science Research Funds of Hefei University under contract No. 17ZR02ZDA and 19ZR02ZDB.

## References

1. K. Tamm, R. Küngas, R.J. Gorte, E. Lust, "Solid oxide fuel cell anodes prepared by infiltration of strontium doped lanthanum vanadate into doped ceria electrolyte", *Electrochim. Acta*, **106** (2013) 398–405.
2. D. Kashyap, P.K. Patro, R.K. Lenka, T. Mahata, P.K. Sinha, "Effects of Gd and Sr co-doping in CeO<sub>2</sub> for electrolyte application in solid oxide fuel cell (SOFC)", *Ceram. Int.*, **40** (2014) 11869–11875.
3. I. Kivi, J. Aruväli, K. Kirsimäe, P. Möller, A. Heinsaar, G. Nurk, E. Lust, "Influence of humidified synthetic air feeding conditions on the stoichiometry of (La<sub>1-x</sub>Sr<sub>x</sub>)<sub>y</sub>CoO<sub>3-δ</sub> and La<sub>0.6</sub>Sr<sub>0.4</sub>Co<sub>0.2</sub>Fe<sub>0.8</sub>O<sub>3-δ</sub> cathodes under applied potential measured by electrochemical in situ high-temperature XRD method", *J. Solid State Electrochem.*, **21** (2016) 361–369.
4. C. Goulart, D. de Souza, "Critical analysis of aqueous tape casting, sintering, and characterization of planar yttria-stabilized zirconia electrolytes for SOFC", *Int. J. Appl. Ceram. Technol.*, **14** (2017) 413–423.
5. S. Kuharungrong, "Ionic conductivity of Sm, Gd, Dy and Er-doped ceria", *J. Power Sources*, **171** (2007) 506–510.
6. K.C. Anjaneya, G.P. Nayaka, J. Manjanna, G. Govindaraj, K.N. Ganesha, "Preparation and characterization of Ce<sub>1-x</sub>Sm<sub>x</sub>O<sub>2-δ</sub> (x = 0.1–0.3) as electrolyte material for intermediate temperature SOFC", *Solid State Sci.*, **26** (2013) 89–96.
7. A. Maheshwari, H.-D. Wiemhöfer, "Sr<sup>2+</sup>-Gd<sup>3+</sup> co-doped CeO<sub>2</sub>: A cost-effective variant for IT-SOFC electrolytes", *Ceram. Int.*, **41** (2015) 9122–9130.
8. M. Dudek, M. Mosiałek, "Utility of Ce<sub>0.8</sub>M<sub>0.2</sub>O<sub>1.9</sub>, Ce<sub>0.8</sub>M<sub>0.15</sub>Y<sub>0.05</sub>O<sub>1.9</sub>, M = Gd, Sm powders synthesized by aerosol decomposition method in solid oxide fuel cell technology", *Electrochim. Acta*, **104** (2013) 339–347.
9. D. Chen, G. Yang, Z. Shao, F. Ciucci, "Nanoscaled Sm-doped CeO<sub>2</sub> buffer layers for intermediate-temperature solid oxide fuel cells", *Electrochem. Commun.*, **35** (2013) 131–134.
10. T. Somekawa, Y. Matsuzaki, Y. Tachikawa, S. Taniguchi, K. Sasaki, "Study of the solid-state reaction at the interface between lanthanoid-doped ceria and yttria-stabilized zirconia for solid-oxide fuel cell applications", *Solid State Ionics*, **282** (2015) 1–6.
11. M. Sahibzada, B.C.H. Steele, K. Hellgardt, D. Barth, A. Effendi, D. Mantzavinos, I.S. Metcalfe, "Intermediate temperature solid oxide fuel cells operated", *Chem. Eng. Sci.*, **55** (2000) 3077–3083.
12. M. Dudek, A. Rapacz-Kmita, M. Mroczkowska, M. Mosiałek, G. Mordarski, "Co-doped ceria-based solid solution in the CeO<sub>2</sub>-M<sub>2</sub>O<sub>3</sub>-CaO, M = Sm, Gd system", *Electrochim. Acta*, **55** (2010) 4387–4394.
13. N. Jaiswal, S. Upadhyay, D. Kumar, O. Parkash, "Ionic conductivity investigation in lanthanum (La) and strontium (Sr) co-doped ceria system", *J. Power Sources*, **222** (2013) 230–236.
14. J.-A. Lee, Y.-E. Lee, H.-C. Lee, Y.-W. Heo, J.-H. Lee, J.-J. Kim, "Effect of Li<sub>2</sub>O content and sintering temperature on the grain growth and electrical properties of Gd-doped CeO<sub>2</sub> ceramics", *Ceram. Int.*, **42** (2016) 11170–11176.
15. E.O. Oh, C.M. Whang, Y.R. Lee, S.Y. Park, D.H. Prasad, K.J. Yoon, J.W. Son, J.H. Lee, H.W. Lee, "Extremely thin bilayer electrolyte for solid oxide fuel cells (SOFCs) fabricated by chemical solution deposition (CSD)", *Adv. Mater.*, **24** (2012) 3373–3377.
16. Y.-C. Wu, C.-C. Lin, "The microstructures and property analysis of aliovalent cations (Sm<sup>3+</sup>, Mg<sup>2+</sup>, Ca<sup>2+</sup>, Sr<sup>2+</sup>, Ba<sup>2+</sup>) co-doped ceria-base electrolytes after an aging treatment", *Int. J. Hydrogen Energy*, **39** (2014) 7988–8001.
17. H. Xu, H. Yan, Z. Chen, "Preparation and properties of Y<sup>3+</sup> and Ca<sup>2+</sup> co-doped ceria electrolyte materials for IT-SOFC", *Solid State Sci.*, **10** (2008) 1179–1184.
18. S.A. Muhammed Ali, M. Anwar, A.M. Abdalla, M.R. Somalu, A. Muchtar, "Ce<sub>0.80</sub>Sm<sub>0.10</sub>Ba<sub>0.05</sub>Er<sub>0.05</sub>O<sub>2-δ</sub> multi-doped ceria electrolyte for intermediate temperature solid oxide fuel cells", *Ceram. Int.*, **43** (2017) 1265–1271.
19. A. Arabaci, V. Sariboğa, M.A.F. Öksüzömer, "Er and Gd co-doped ceria-based electrolyte materials for IT-SOFCs prepared by the cellulose-templating method", *Metal. Mater. Trans. A*, **45** (2014) 5259–5269.
20. C.G.M. Lima, T.H. Santos, J.P.F. Grilo, R.P.S. Dutra, R.M. Nascimento, S. Rajesh, F.C. Fonseca, D.A. Macedo, "Synthesis and properties of CuO-doped Ce<sub>0.9</sub>Gd<sub>0.1</sub>O<sub>2-δ</sub> electrolytes for SOFCs", *Ceram. Int.*, **41** (2015) 4161–4168.
21. E.Y. Pikalova, A.A. Murashkina, V.I. Maragou, A.K. Demin, V.N. Strelakovsky, P.E. Tsiakaras, "CeO<sub>2</sub> based materials doped with lanthanides for applications in intermediate temperature electrochemical devices", *Int. J. Hydrogen Energy*, **36** (2011) 6175–6183.
22. B. Matović, M. Stojmenović, J. Pantić, A. Varela, M. Žunić, N. Jiraborvornpongsa, T. Yano, "Electrical and microstructural properties of Yb-doped CeO<sub>2</sub>", *J. Asian Ceram. Soc.*, **2** (2014) 117–122.
23. R.D. Shannon, "Revised effective ionic radii and systematic studies of interatomic distances in halides and chalcogenides", *Acta Cryst.*, **A32** (1976) 751–767.
24. K.C. Anjaneya, G.P. Nayaka, J. Manjanna, G. Govindaraj, K.N. Ganesha, "Preparation and characterization of Ce<sub>1-x</sub>Gd<sub>x</sub>O<sub>2-δ</sub> (x = 0.1–0.3) as solid electrolyte for intermediate temperature SOFC", *J. Alloys Compd.*, **578** (2013) 53–59.
25. R.K. Lenka, T. Mahata, A.K. Tyagi, P.K. Sinha, "Influence

- of grain size on the bulk and grain boundary ion conduction behavior in gadolinia-doped ceria”, *Solid State Ionics*, **181** (2010) 262–267.
26. L. Ge, R. Li, S. He, H. Chen, L. Guo, “Enhanced grain-boundary conduction in polycrystalline  $\text{Ce}_{0.8}\text{Gd}_{0.2}\text{O}_{1.9}$  by zinc oxide doping: Scavenging of resistive impurities”, *J. Power Sources*, **230** (2013) 161–168.
27. W. Shen, J. Jiang, C. Ni, Z. Voras, T.P. Beebe, J.L. Hertz, “Two-dimensional vacancy trapping in yttria doped ceria”, *Solid State Ionics*, **255** (2014) 13–20.
28. D. Zhou, Y. Xia, J. Zhu, W. Guo, J. Meng, “Preparation and electrical properties of new oxide ion conductors  $\text{Ce}_{6-x}\text{Gd}_x\text{MoO}_{15-\delta}$  ( $0.0 \leq x \leq 1.8$ )”, *J. Am. Ceram. Soc.*, **92** (2009) 1042–1046.